

Large Scale Structure in the ELAIS S1 Survey

E. A. Gonzalez-Solares^{1,2*}, S. Oliver¹, C. Gruppioni^{3,4}, F. Pozzi^{4,5} C. Lari⁶
 M. Rowan-Robinson⁷, S. Serjeant⁸, F. La Franca⁹, M. Vaccari⁷

¹*Astronomy Centre, Department of Physics and Astronomy, University of Sussex, Falmer, Brighton BN1 9RH*

²*University of Cambridge, Institute of Astronomy, The Observatories, Madingley Road, Cambridge CB3 0HA*

³*Istituto Nazionale di Astrofisica, Osservatorio Astronomico di Padova, vicolo dell’Osservatorio 5, I-35122 Padova, Italy*

⁴*Istituto Nazionale di Astrofisica, Osservatorio Astronomico di Bologna, via Ranzani 1, I-40127 Bologna, Italy*

⁵*Dipartimento di Astronomia, Università di Bologna, via Ranzani 1, I-40127 Bologna, Italy*

⁶*Istituto di Radioastronomia del CNR, via Gobetti 101, I-40129 Bologna, Italy*

⁷*Astrophysics Group, Blackett Laboratory, Imperial College of Science, Technology & Medicine, Prince Consort Road, London SW7 2BZ*

⁸*Centre for Astrophysics and Planetary Science, School of Physical Sciences, University of Kent, Canterbury, Kent, CT2 7NR*

⁹*Dipartimento di Astronomia, Università degli Studi “Roma TRE”, Via della Vasca Navale 84, I-00146, Roma, Italy*

ABSTRACT

We present an analysis of the two-point angular correlation function of the ELAIS S1 survey. The survey covers 4 deg² and contains 462 sources detected at 15 μ m to a 5 σ flux limit of 0.45 mJy. Using the 329 extragalactic sources not repeated in different observations, we detect a significant clustering signal; the resulting angular correlation function can be fitted by a exponential law $w(\theta) = A\theta^{1-\gamma}$ with $A = 0.014 \pm 0.005$ and $\gamma = 2.04 \pm 0.18$. Assuming a redshift distribution of the objects, we invert Limber’s equation and deduce a spatial correlation length $r_0 = 4.3_{-0.7}^{+0.4} h^{-1}$ Mpc. This is smaller than that obtained from optical surveys but it is in agreement with results from IRAS. This extends to higher redshift the observational evidence that infrared selected surveys show smaller correlation lengths (i.e. reduced clustering amplitudes) than optical surveys.

Key words: galaxies: clusters: general – galaxies: evolution – infrared: galaxies – cosmology: observations – large-scale structure of Universe

1 INTRODUCTION

Theories of structure formation were strongly constrained by the statistical measurements of clustering in some of the early galaxy redshift surveys. Surveys of infrared galaxies, in particular, were able to rule out the then standard Cold Dark Matter Model (Efstathiou et al. 1990; Saunders et al. 1991). Present day redshift surveys such as the 2dFGRS (Colless et al. 2001), SDSS (York et al. 2000) and, in the far-infrared, the Point Source Catalog Redshift survey, PSC-z (Saunders et al. 2000) are now able to provide definitive measurements of the galaxy clustering in the local Universe.

Despite this success, we have always known that galaxies are biased tracers of the matter distribution and yet we have a poor observational or theoretical understanding of this bias, although it is assumed to be related to the process of galaxy formation and evolution. To understand bias and, by inference, galaxy formation, we need to better understand the clustering of different galaxy types and the evolution of this clustering with redshift.

In this paper we attempt to provide an estimate of the

clustering of infrared galaxies a factor of ten deeper (in redshift) than those seen in the IRAS surveys. To do this we provide the first estimate of clustering from any of the extragalactic ISO surveys. This is thus the first estimate of clustering from galaxies selected at 15 μ m. We have used part of the ELAIS survey (Oliver et al. 2000) as this probes the largest volume of any of the ISO surveys. We measure the projected clustering by calculating the angular correlation function, we then discuss the constraints this places on the three dimensional clustering using Limber’s equation.

2 THE ELAIS S1 SURVEY

The European Large-Area ISO survey (ELAIS, Oliver et al. 2000) was the largest Open Time programme on ISO. This project surveyed 12 square degrees, larger than all but the serendipitous surveys, making it ideal for clustering studies. The main survey bands were at 6.7, 15, 90 and 170 μ m. Of these bands the 15 μ m catalogues contain the greatest density of galaxies (see e.g. Gruppioni et al. 2002; Serjeant et al. 2000), and provide the best statistics for clustering. The final analysis of the 15 μ m data using the Lari method for

* E-mail: eglez@ast.cam.ac.uk

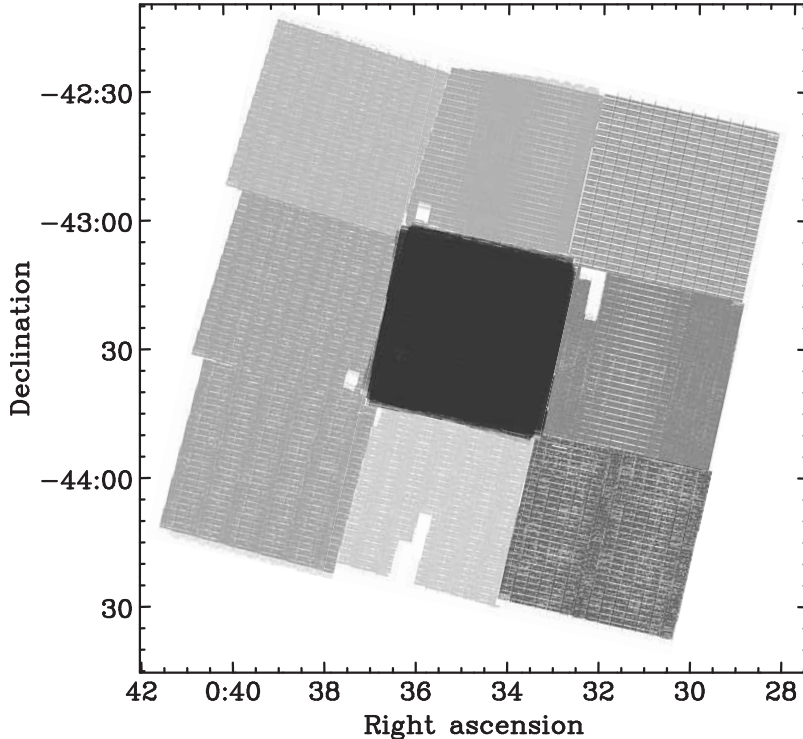


Figure 1. Selection function used to generate the random sample of galaxies. The dark central region arises due to the deeper observations carried out in.

one of the ELAIS fields (S1) has recently been completed (Lari et al. 2001) and this is the sample that we use in this analysis.

The S1 field is located at $\alpha(2000) = 00^h 34^m 44.4^s$, $\delta(2000) = -43^\circ 28' 12''$, covering an area of 2×2 square degrees. The $15\mu\text{m}$ survey is made from 9 raster observations, each one of $\sim 40' \times 40'$. The central raster S1.5 has been observed three times. Using the Lari method we have obtained a sample of 462 sources to 5σ in the flux range 0.45-150 mJy (Gruppioni et al. 2002).

3 SELECTION FUNCTION

Besides the galaxy catalogue itself, the selection function is the most important ingredient in the calculation of clustering statistics. Errors in the selection function will invalidate the answer, whereas errors in the weighting scheme will usually make the answer more noisy.

A selection function is required for each source list that is being investigated. The selection function, ϕ , is defined as the expected number density of sources as a function of \mathbf{r} (which might be two or three dimensional), in absence of clustering; i.e., the expected number of galaxies $d\mathcal{N}$ in a volume dV is $d\mathcal{N} = \phi(\mathbf{r})dV$. With this definition, $\int \phi(\mathbf{r})dV = \mathcal{N}$. The selection function is used to simulate a catalogue with no clustering.

To be selected from the ELAIS S1 catalogue sources had to exceed a signal-to-noise threshold, σ_{min} . The signal to noise of a detected source i , is $\sigma_i(\mathbf{r}_i) = S_i/N(\mathbf{r}_i)$ where S_i is the signal of the source and $N(\mathbf{r}_i)$ is the noise at the position of the source. Had this source been in a different

part of the survey, \mathbf{r} it would have had a different signal-to-noise. We can define then a mask, $M_i(\mathbf{r})$, which represents the detectability of each object as a function of position as follows

$$M_i(\mathbf{r}) = \begin{cases} 0 & \text{if } \sigma_i(\mathbf{r}) < \sigma_{min} \\ 1 & \text{if } \sigma_i(\mathbf{r}) \geq \sigma_{min} \end{cases} \quad (1)$$

where $\sigma_{min} = 5$. The un-normalised selection function can then be written as

$$\phi' = \sum_i M_i(\mathbf{r}) \quad (2)$$

which can be normalised

$$\phi = \phi' \frac{\mathcal{N}}{\int \phi' dV} \quad (3)$$

3.1 Building the masks

In the full ELAIS S1 region there are 9 independent noise maps $N(\mathbf{r})$, corresponding to 9 independent sub-catalogues. Note that the central noise map is less noisy and the corresponding sub-catalogue deeper, because the ISO data were already combined (Gruppioni et al. 2002). We constructed a selection function as follows: for each source in the sub-catalogue we calculate the hypothetical signal-to-noise ratio (defined as the peak flux over the rms value) at each point in the raster. Where these exceed the extraction signal-to-noise threshold σ_{min} (equation 1), the value of the selection function at that position is incremented (equation 2).

The 9 individual selection functions are then combined into a single one. Figure 1 shows the final image. In the overlap region only one selection function was used and the final

catalogue excludes sources in that region that arose from the other sub-catalogues. Sources with stellar counterparts have also been removed (see Gruppioni et al. 2002) from the catalogue and excluded from the calculation of the selection function. We end up with a catalogue of 329 sources.

The selection function so obtained is then used to generate the random catalogues with no clustering, essential to properly calculate the two point correlation function.

4 THE ANGULAR CORRELATION FUNCTION

Correlation functions are widely used to study the distribution of sources in surveys and to derive large scale properties of galaxies. The two-point spatial correlation function is defined so that

$$dP = n^2[1 + \xi(r)]dV_1dV_2$$

is the joint probability of finding a source in a volume element dV_1 and another source in a volume element dV_2 . The function $\xi(r)$ is the excess probability of finding an object compared to a random distribution of objects.

Similarly, one can define the two point angular correlation function so that

$$dP = n^2[1 + w(\theta)]d\Omega_1d\Omega_2$$

is the joint probability of finding a source in a solid angle element $d\Omega_1$ and another source in a solid angle element $d\Omega_2$. These two statistics are related by Limber's equation (Peebles 1980).

In order to calculate the angular correlation function of mid-IR sources we use the Landy & Szalay estimator (Landy & Szalay 1993)

$$w(\theta) = \frac{[DD] - 2[DR] + [RR]}{[RR]} \quad (4)$$

where [DD], [RR] and [DR] represents the normalized number of galaxy-galaxy, random-random and galaxy-random pairs with angular separation in $(\theta, \theta + d\theta)$.

Errors in the calculation of the angular correlation function are dominated by Poisson noise. The error in each bin can be estimated using the following expresion (Baugh et al. 1996b):

$$\delta w(\theta) = 2\sqrt{\frac{1 + w(\theta)}{DD}} \quad (5)$$

where, in this case, DD is the total number of galaxy-galaxy pairs (not normalized). Errors calculated using this equation are comparable to the errors obtained from a bootstrap resampling technique (Ling, Barrow, & Frenk 1986).

A second source of errors comes from the to finite size of the sample. In order to correct for this effect we use the random sample to calculate the integral constraint as (e.g. Infante et al. 1994)

$$\delta = \frac{\sum N_{rr}(\theta)}{\sum N_{rr}(\theta)(1 + w(\theta))} \quad (6)$$

and divide the calculated correlation function by this factor, $\delta = 0.945$.

Figure 2 (top) shows the obtained angular correlation function, calculated using 200 realizations with 2000 random

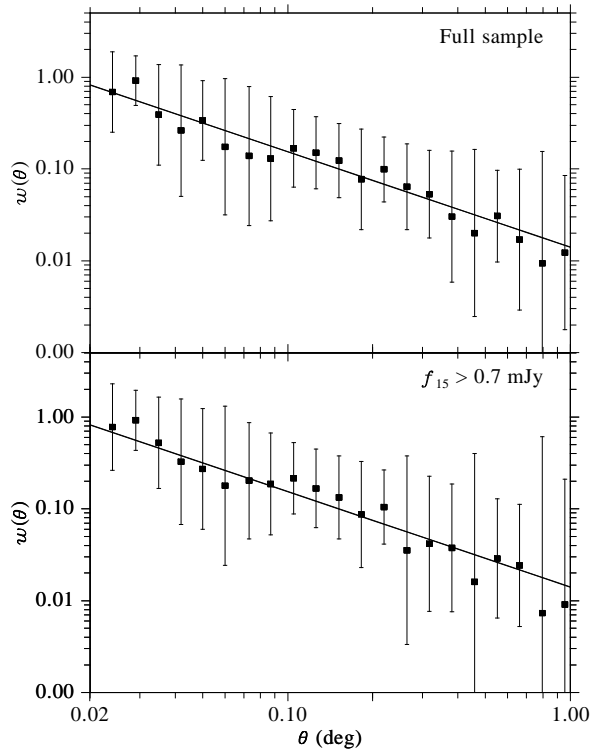


Figure 2. Angular correlation function as calculated from ELAIS S1. Top figure shows the calculation performed using all sources, while in the bottom figure only those sources with fluxes larger than 0.7 mJy have been considered (excluding then, those faint sources only detectable in the central deeper raster S1_5). Data points are fitted by a exponential law $w(\theta) = A\theta^{1-\gamma}$ with $A = 0.014 \pm 0.005$ and $\gamma = 2.04 \pm 0.18$.

sources each, in intervals of $\log \theta = 0.08$ degrees. Random catalogues have been built using the selection function calculated in previous section. Data points have been fitted by an exponential law of the form $w(\theta) = A\theta^{1-\gamma}$ resulting in $A = 0.014 \pm 0.005$ and $\gamma = 2.04 \pm 0.18$ (where θ is measured in degrees).

The mean number of objects in each field is $\langle n \rangle = 35.25$ (excluding the central raster S1_5, with 71 sources), with a standard deviation of 6 objects. Since S1_5 field reaches deeper flux limits, it could in principle be subject to clustering variations that would affect the whole clustering estimation. We repeat the above calculation removing those sources with fluxes fainter than the flux limit excluding S1_5: a total of 27 sources with fluxes lower than 0.7 mJy are removed. By calculating again the selection function and the angular correlation function we obtain then an estimate of the clustering from sources detectable over most of the S1 field. In this case the integral constraint is slightly larger than the previously obtained, $\delta = 0.970$. The angular correlation function is shown in figure 2 (bottom) and is fitted by the same exponential law previously calculated. Although the correlation function is now slightly larger at scales ~ 0.1 deg, the errors are also larger and the overall correlation function is well fitted by the previous function.

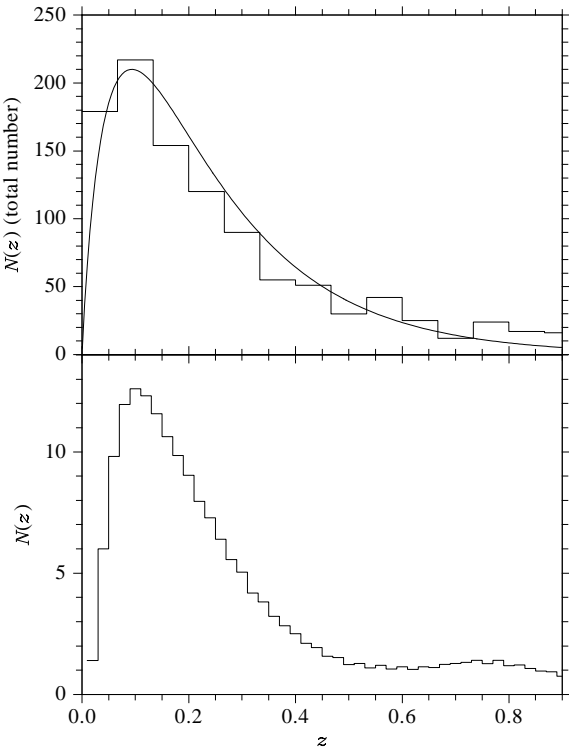


Figure 3. Top: Redshift distribution of ELAIS objects obtained from followup spectroscopic observations and photometric redshifts. Bottom: Model redshift distribution of ELAIS sources obtained by Pozzi et al. (2004).

5 SPATIAL CORRELATION FUNCTION

In case of small angles, both w and ξ can be approximated by power law shapes, and the spatial correlation function can be written as (e.g., Phillipps et al. 1978)

$$\xi(r, z) = \left(\frac{r}{r_0}\right)^{-\gamma} (1+z)^{-(3+\epsilon)} \quad (7)$$

where r_0 is the comoving correlation length at $z = 0$ and r the comoving distance. The parameter ϵ is the clustering evolution index and is interpreted as follows. A value $\epsilon = 0$ corresponds to stable clustering in physical coordinates, i.e., galaxy clusters remain unchanged and clustering changes due to the expansion of the Universe, while $\epsilon = 3 - \gamma$ corresponds to clustering fixed in comoving coordinates, i.e., clustering does not change with time and the galaxy clusters expand with the Universe.

If $w(\theta)$ is parametrized as $w(\theta) = A_w \theta^{1-\gamma}$, then Limber's equation becomes (e.g., Phillipps et al. 1978)

$$A_w = Cr_0^\gamma \frac{\int D_\theta^{1-\gamma} g^{-1}(z) (1+z)^{-(3+\epsilon)} (dN/dz)^2 dz}{(\int (dN/dz) dz)^2} \quad (8)$$

where D_θ is the angular diameter distance, $g(z)$ is the scale factor multiplied by the element of comoving distance

$$g(z) = \frac{c}{H_0} [(1+z)^2 (1+\Omega_0 z)^{1/2}]^{-1} \quad (9)$$

and

$$C = \pi^{1/2} \frac{\Gamma[(\gamma-1)/2]}{\Gamma(\gamma/2)} \quad (10)$$

The only unknown quantity in equation 8 is the redshift distribution of the sources. A distribution given by

$$\frac{dN}{dz} = \frac{3\mathcal{N}\Omega_s}{2z_c^3} z^2 \exp\left[-\left(\frac{z}{z_c}\right)^{3/2}\right]$$

where $z_m = \sqrt{2}z_c$ is the median redshift of the survey, provides good fits to the distribution of optical galaxies (Baugh 1996a, and references therein) and as been widely used to invert Limber's equation. However, the redshift distribution of mid-IR sources is more extended and the equation above is no longer valid. Figure 3 (top) shows the redshift distribution of the ELAIS sources, obtained from optical spectroscopy (La Franca et al. 2004, in prep; Perez-Fournon et al. 2004, in prep) and photometric redshifts (Rowan-Robinson et al. 2003). Instead of the optical dN/dz we use

$$\frac{dN}{dz} \propto z \exp\left[-\left(\frac{z}{z_c}\right)^{3/4}\right] \quad (11)$$

which fits reasonably well the distribution of ELAIS sources.

We can now integrate equation 8 in order to obtain r_0 . Assuming $\Omega_0 = 1.0$ and $\epsilon = 0$ and using a median redshift of $z_m = 0.1$ in equation 11, we obtain $r_0 = 4.3 h^{-1}$ Mpc with a 95% confidence level in the range $3.8 h^{-1}$ Mpc to $4.7 h^{-1}$ Mpc.

An alternative redshift distribution of the ELAIS sources has been presented by Pozzi et al. (2004), computed from the luminosity function fit of galaxies on ELAIS S1 and S2 (see figure 3 – bottom). When using this redshift distribution as input to equation 8 we obtain similar results of $r_0 = 4.2 h^{-1}$ Mpc with a 95% confidence level in the range $3.6 h^{-1}$ Mpc to $4.8 h^{-1}$ Mpc.

6 DISCUSSION

We use a sample of 329 15μm galaxies detected in the ELAIS S1 survey covering a region of 4 square degrees of sky to determine the angular correlation function of the galaxies. We measure $w(\theta)$ up to scales of 1 degree, corresponding to ~ 7 Mpc at the mean redshift of $z = 0.14$. The resulting correlation function is well fitted by a power law $w(\theta) = A\theta^{1-\gamma}$ with $A = 0.014 \pm 0.005$ and $\gamma = 2.04 \pm 0.18$. Assuming a redshift distribution we invert the angular correlation using Limber's equation in order to determine the correlation length r_0 . We find a value of $r_0 = 4.3 h^{-1}$ Mpc with a 95% confidence level in the range $3.8 h^{-1}$ Mpc to $4.7 h^{-1}$ Mpc.

Table 1 lists the correlation lengths obtained from several optical and infrared surveys. While optical surveys show a significant clustering with $r_0 \sim 5 h^{-1}$ Mpc, IRAS survey shows a lower value. The data described in this paper is consistent with this trend: that mid infrared selected sources show a smaller correlation length. This is expected because optical surveys favour elliptical galaxies which are more strongly clustered than spiral galaxies, while infrared surveys preferentially select spirals and star-forming galaxies. We note that the ELAIS selected galaxies appear to have a marginally steeper two point correlation function than the optical and the IRAS surveys. By fixing γ to the lower value allowed by the fit $\gamma = 1.86$ we obtain $r_0 = 4.1^{+0.2}_{-0.5}$, bringing the clustering amplitude closer to that seen by IRAS.

Table 1. Summary of correlation lengths values obtained from different surveys.

Survey	z_m	r_0	γ	Ref.
APM	0.05	5.7	1.67	1
SDSS	0.18	5.7 ± 0.2	1.75 ± 0.03	2
2dFGRS	0.08	4.92 ± 0.27	1.71 ± 0.06	3
IRAS	0.02	3.79 ± 0.14	1.57 ± 0.03	4
PSCz	0.02	3.7	1.69	5
ELAIS	0.14	$4.2^{+0.4}_{-0.7}$	2.04 ± 0.18	

References: 1 Maddox et al. 1990; 2 Zehavi et al. 2002 (assuming a Einstein-de Sitter cosmology); 3 Norberg et al. 2001; 4 Saunders et al. 1992; 5 Jing et al. 2002

It is interesting to note that the optical correlation function at $z \sim 0.2$ (Zehavi et al. 2002; Norberg et al. 2001) is consistent with that at $z \sim 0$ (Maddox et al. 1990), i.e. there is no apparent evolution in the correlation function over this albeit small redshift range. Likewise the infrared galaxy correlation function estimate from this work at $z \sim 0.14$ is consistent with the infrared galaxy correlation function estimated from IRAS galaxies at $z = 0$ (Jing et al. 2002). This apparent lack of evolution may be because evolutionary effects are small or that evolution in mass clustering is compensated by evolution in galaxy bias. It will be interesting to see if this apparent non-evolution in clustering of different galaxy population mixes is still found in deeper surveys (e.g. SWIRE, Lonsdale et al. 2003) as this might imply a striking conspiracy in the evolution of the bias in different galaxy types.

By performing a systematic analysis of all density peaks in the redshift distribution of field galaxies, Elbaz & Moy (2004) recently found an excess of ISO selected galaxies over the whole range of density peaks. This suggests that infrared galaxies are more strongly clustered than optical galaxies, in apparent contradiction to our results. Since the ISO-CAM surveys are deeper than ELAIS, it is plausible that there is an evolution of the clustering over the redshift interval spanned by these two ISO surveys. Infrared galaxies would then become more clustered towards higher redshift, while the clustering of optical galaxies changes little. This would agree qualitatively with hierarchical pictures of structure formation. Such models predict that star formation and galaxy formation is driven by merger rate that would be a function of environment. Star formation would thus have occurred first and vigorously in the denser (more clustered) regions of the Universe, taking more time to initiate in lower density (less clustered) regions (see also Elbaz & Cesarsky 2003). The strong evolution in luminosity function of infrared galaxies (e.g. Pozzi et al. 2004) might then be coupled with an evolution in their clustering. Optically selected galaxies sample regions where past star formation activity was high as well as those where current activity is high and are thus less sensitive to these effects. Finally this apparent contradiction may simple be that the deep ISO-CAM surveys do not sample a sufficiently large volume to be representative of the rest of the Universe.

7 ACKNOWLEDGEMENTS

Eduardo Gonzalez-Solares was supported by PPARC grant PPA/G/S/2000/00508 and EC Marie Curie Fellowship MCFI-2001-01809. This paper is based on observations with *ISO*, an ESA project, with instruments funded by ESA Member States (especially the PI countries: France, Germany, the Netherlands and the United Kingdom) and with participation of ISAS and NASA. Some of this work was supported by EEC Training Mobility Research Network "Probing the Origin of the Extra-galactic background light" (POE) HPRN-CT-2000-00138. The author also wants to thank D. Elbaz for useful comments on the discussion of the results presented.

REFERENCES

Baugh C. M., 1996, MNRAS, 280, 267
 Baugh C. M., Gardner J. P., Frenk C. S., Sharples R. M., 1996, MNRAS, 283, L15
 Colless M. et al., 2001, MNRAS, 328, 1039
 Efstathiou G., Kaiser N., Saunders W., Lawrence A., Rowan-Robinson M., Ellis R. S., Frenk C. S., 1990, MNRAS, 247, 10P
 Elbaz D., Moy E., 2004, astro-ph/0401617
 Elbaz D., Cesarsky C. J., 2003, Science, 300, 270
 Gruppioni C., Lari C., Pozzi F., Zamorani G., Franceschini A., Oliver S., Rowan-Robinson M., Serjeant S., 2002, MNRAS, 335, 831
 Jing, Y. P., Börner, G., & Suto, Y. 2002, ApJ, 564, 15
 Landy S. D., Szalay A. S., 1993, ApJ, 412, 64
 Lari C. et al., 2001, MNRAS, 325, 1173
 Ling E. N., Barrow J. D., Frenk C. S., 1986, MNRAS, 223, 21P
 Lonsdale C. J. et al., 2003, PASP, 115, 897
 Maddox S. J., Efstathiou G., Sutherland W. J., Loveday J., 1990, MNRAS, 242, 43P
 Norberg P. et al., 2001, MNRAS, 328, 64
 Peebles P. J. E., 1980
 Phillipps S., Fong R., Fall R. S. E. S. M., MacGillivray H. T., 1978, MNRAS, 182, 673
 Pozzi F. et al., 2004, AJ, submitted
 Rowan-Robinson M. et al., 2003, astro-ph/0308283
 Saunders W., Frenk C., Rowan-Robinson M., Lawrence A., Efstathiou G., 1991, Nature, 349, 32
 Saunders W., Rowan-Robinson M., Lawrence A., 1992, MNRAS, 258, 134
 Saunders W. et al., 2000, MNRAS, 317, 55
 Serjeant S. et al., 2000, MNRAS, 316, 768
 York D. G., Adelman J., Anderson J. E., et al., 2000, AJ, 120, 1579
 Zehavi I., Blanton M. R., Frieman J. A., et al., 2002, ApJ, 571, 172